

Compact Single Notch UWB Bandpass Filter with Metamaterial and SIW Technique

Senathipathi Udhayanan and Krishnan Shambavi*

School of Electronics Engineering, Vellore Institute of Technology, Vellore, India

ABSTRACT: A design of a compact planar SIW filter with notch band characteristics is proposed. Double split square complementary split ring resonators are used to realize the ultra-wideband (UWB) characteristics. Proposed UWB filter contributes a passband from 2.9 GHz to 10.3 GHz with minimum insertion loss 0.7 dB at 3.7 GHz and maximum of 1.84 dB at 7 GHz. By employing a complementary split ring resonator in the ground plane, a narrow band characteristic is obtained to reject the undesired wireless local area network (WLAN) signals. The notch band frequency ranges from 5 GHz to 5.7 GHz with insertion loss of 14 dB at center frequency. The 3 dB fractional bandwidth in the notch band is 12.9%. The variation of group delay is less than 0.5 ns in the passband range. Overall size of the proposed filter is $0.35\lambda_g \times 1.06\lambda_g$. Because of these salient features, the proposed filter can be used for space applications.

1. INTRODUCTION

Recently, ultra-wideband (UWB) technology has become increasingly popular due to its high-speed data transfer, high channel capacity, and reliable communications for markets like telecommunications, aerospace, and defense [1]. UWB bandpass filters were designed to remove noise and unwanted signals in UWB applications, and UWB spectrum is prone to interfere with WLAN, WIFI, RFID, etc. Nowadays, researchers mainly focused to develop a compact and low-profile notched band bandpass filters with easy-to-integrate existing applications. These notch filters can be implemented using different transmission lines, like microstrip lines, strip lines, rectangular waveguides, etc. [2, 3]. Microstrip notch filters have different techniques like open circuited stub, meander line slot multi-mode resonator with parasitic coupled line, etc. [4]. But the mentioned filters suffer from high radiation loss and ohmic loss, which leads to high insertion loss in the passband. Furthermore, the quality factor is also not reasonable compared to a traditional rectangular waveguide. The substrate-integrated waveguide circuit with complementary split-ring resonator elements are capable of achieving high quality factors, high-power handling capability, and easy integration with planar components [5, 6]. To achieve compactness and improve the performance standard of the microwave filters, metamaterials such as split ring resonator (SRR) and complementary SRR (CSRR) are added to substrate integrated waveguide (SIW). SRR has negative permeability, and the complementary structure of SRR, i.e., CSRR, provides negative permittivity near its resonance frequency, hence providing a sharp rejection band [7]. Furthermore, in SRR-loaded waveguide, according to the theory of evanescent mode, the additional passband below the cutoff can be obtained by loading CSRRs. Using SRRs, many single and dual-band filters have been implemented.

The CSRR-loaded notched bandpass filters were reported in [8–10] to miniaturize the filter structure. The CSRR carved on a ground plane under signal path leads to stopband behaviors reported in [11–14].

In this brief, a SIW-based UWB notch band bandpass filter designed using a dual-split square complementary split ring resonator (DSS-CSRR) and conventional CSRR defected ground structure is presented. The DSS-CSRR was etched on the top and bottom layers to obtain the required passband characteristics and to improve the selectivity of the filter. A notched band is created and controlled using CSRR defected ground structure. The slots were introduced in the ground plane to compensate the impedance variation. The designed filter contributes low insertion loss in the operating band. Hence, it is well suited for space applications.

2. DESIGN AND ANALYSIS OF SIW FILTER

2.1. Design of SIW

Substrate integrated waveguide and conventional rectangular waveguide have similar wave and mode characteristics and behave like a high pass filter when unloaded. Its cutoff frequency depends on the effective separation between the two-side walls W_W and the dielectric material on which it is realized. Using Equations (1) and (2), SIW filter was designed for an FR4 substrate and validated using CST software. To obtain the desired passband characteristics, SIW is loaded with a novel DSS-CSRR to control the band edge characteristics of the filter and to reject the upper WLAN frequency. A circular CSRR is carved on a ground plane. The inherent characteristics of the CSRRs are shown in Figure 3. The CSRR provides a negative permittivity at resonance frequency and generates an abrupt rejection band around the designed frequency.

$$f_c = \frac{c}{2W_W\sqrt{\epsilon_r}} \quad (1)$$

* Corresponding author: Krishnan Shambavi (kshambavi@vit.ac.in).

$$W_W = W - 1.08 \frac{d^2}{S} + 0.1 \frac{d^2}{W} \quad (2)$$

In SIW, periodic vias are utilized to realize the side walls, and the separation between the vias (s) and via diameter (d) should obey $d/s \geq 0.5$, $d/\lambda_c \leq 0.125$ to minimize the leakage loss, where λ_c is the cutoff wavelength of the waveguide. Figure 1 shows the isometric view of proposed notch filter.

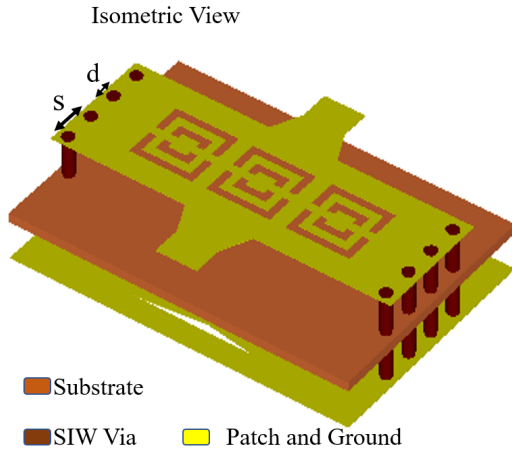


FIGURE 1. Isometric view of proposed notch filter.

2.2. Design of CSRR

CSRR provides a negative permittivity at resonance frequency and generates an abrupt rejection band around the designed frequency. In this proposed SIW filter, a novel dual-split square CSRR of 8.45 GHz resonant frequency is implemented to obtain the desired wideband characteristics. A dual-split square CSRR is etched on an FR-4 substrate. The optimized dimensions are $W_{CSRR} = L_{CSRR} = 7.5$ mm, $R = 2.2$ mm, $S = 4.2$ mm, $g_1 = g_2 = g_3 = 0.5$ mm, $R_1 = 2.7$ mm, $R_2 = 1.7$ mm. To validate the design, DSS-CSRR is simulated using CST software. The band reject frequency of the unit cell is 8.45 GHz, and its negative permittivity is high at the resonant frequency. By incorporating this resonator into the unloaded SIW filter, the band edge characteristics of the bandpass filter can be tuned to obtain the required bandwidth. The notch band is obtained by the circular CSRR carved on a ground plane, under the signal path. Due to the negative effective permittivity (5.38–5.64 GHz) in the proximity of CSRR resonance, the sig-

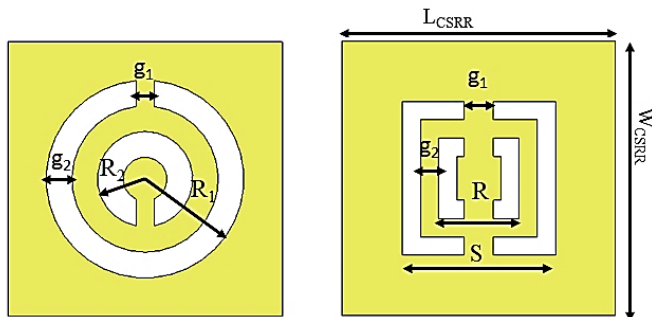


FIGURE 2. Schematic diagram of square CSRR and circular CSRR.

nal is inhibited from 5 to 5.7 GHz. Figures 2 and 3 depict the schematic and relative permittivity of dual-split square CSRR and circular CSRR.

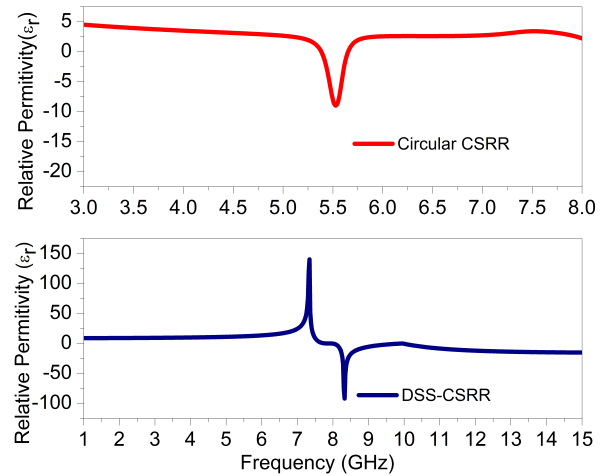


FIGURE 3. Relative permittivity of square and circular CSRRs.

2.3. Design and Analysis of Proposed UWB Notch Filter

The SIW filter is fed by a tapered transition to a 50 Ω microstrip line. The width of the tapered transmission line depends on the waveguide impedance (3), and its length corresponds to quarter wavelength of the filter in order to maintain impedance matching.

$$Z = \frac{60}{\sqrt{\epsilon_e}} \ln \left(8 \frac{h}{T_w} + 0.25 \frac{T_w}{h} \right) \quad (3)$$

where Z denotes the waveguide impedance, and T_w represents the flaring width. CSRRs etched on the top and bottom layers to control the upper band edge characteristics. Slots are etched in the bottom layer to improve the return loss and insertion loss characteristics of the filter. Figure 4 shows the methodology and frequency response characteristics of proposed UWB filter.

Loading a SIW with dual split-CSRR on the top layer exhibits wide passband characteristics with 3 dB cutoff frequencies of 3.1 GHz and 13.2 GHz (Figure 4(a)). Adding a CSRR to the ground plane (Figure 4(b)) changes the filter’s resonance frequency by lowering the upper cutoff frequency of the passband from 13.2 GHz to 10.5 GHz. Loading CSRRs in the top and bottom layers of SIW changes the impedance of the filter, which in turn affects the return loss and insertion loss characteristics. Hence, the slots are etched in the ground plane to compensate the variation (Figure 4(c)). The circular CSRR is implemented in the ground plane to create a notch band characteristic. The 3 dB notch band frequency range is from 5 GHz to 5.7 GHz. By modifying the dimensions of CSRR, the notch width and position can be easily adjusted, as shown in Figure 5. The simulated notch band has the center frequency of 5.4 GHz with 14 dB insertion loss and 3 dB fractional bandwidth of 12.9%. The proposed notch filter is mainly designed to eliminate the interference from WLAN applications. A triangular slot in the ground plane enhances the stopband attenuation

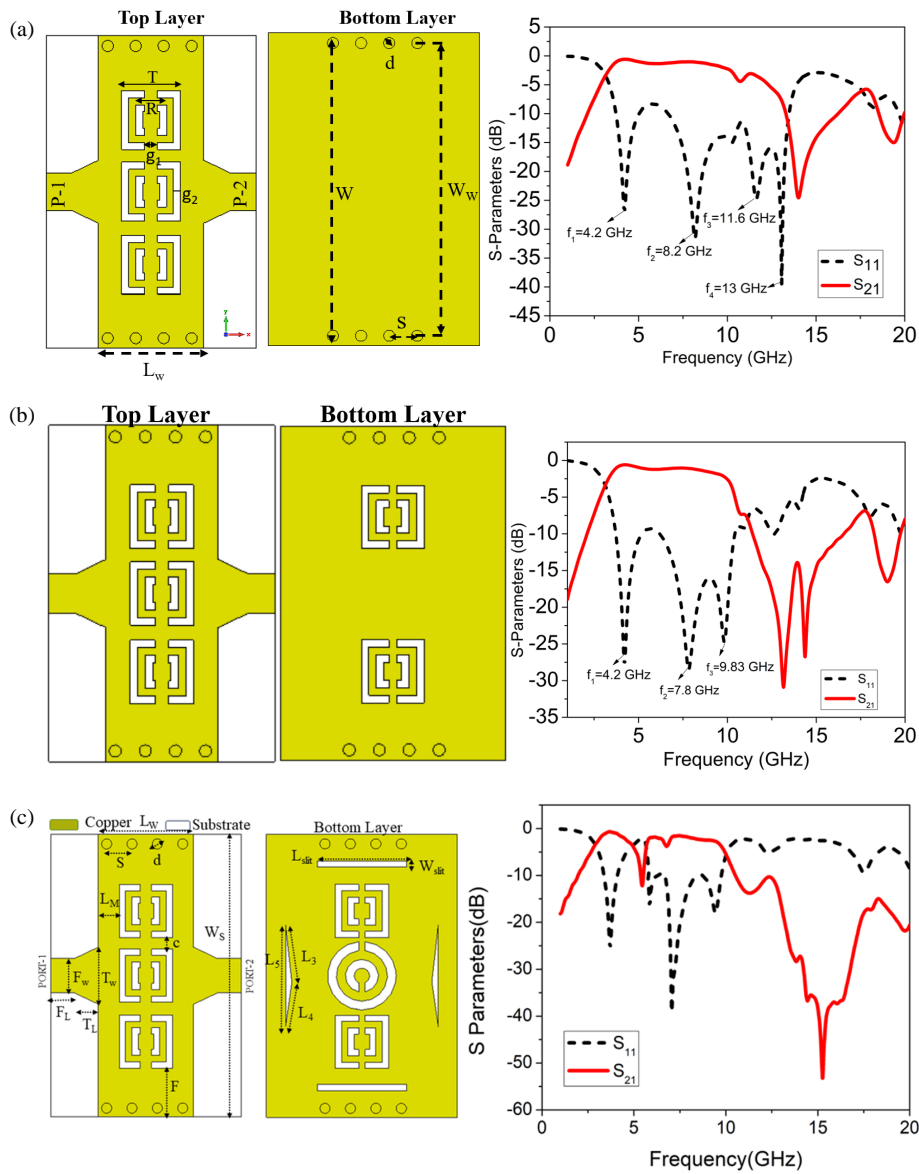


FIGURE 4. Design steps and corresponding simulation results of proposed UWB bandpass filter. The optimized dimensions of the designed filter are $F_w = 2.7$, $F_L = 1.85$, $T_L = 1.90$, $T_w = 4.4$, $L_M = 1.7$, $L_W = 7.5$, $L_s = 15$, $W_S = 22.3$, $F = 3.8$, $c = 1$, $W_{slit} = 0.5$, $s = 2$, $d = 0.8$, $L_3 = 4.53$, $L_4 = 3.54$, $L_5 = 8$, $L_{slit} = 6.8$, $R = 2.2$ mm, $T = 4.2$ mm, $g_1 = g_2 = g_3 = 0.5$ mm, $R_1 = 2.7$ mm, $R_2 = 1.3$ mm, $W = 20.88$, $W_W = 20.08$ and substrate $h = 1.6$, $\epsilon_r = 4.3$ respectively. (Unit: mm).

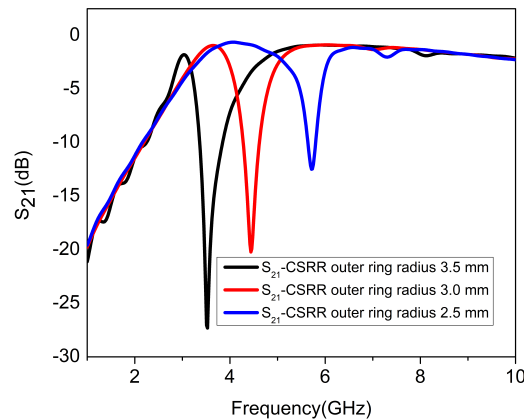


FIGURE 5. S_{21} characteristics of varying CSRR dimensions.

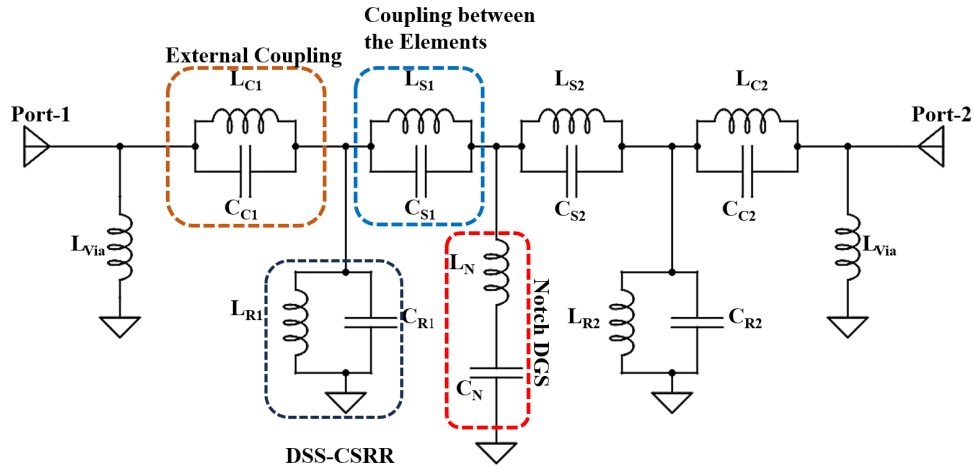


FIGURE 6. Equivalent circuit model of proposed UWB notch filter. The electrical parameters are: $L_{C1} = 2.48$ nH, $C_{C1} = 2.643$ pF, $L_{S1} = 0.337$ nH, $C_{S1} = 0.322$ pF, $L_{C2} = 2.47$ nH, $C_{C2} = 2.555$ pF, $L_{S2} = 0.3062$ nH, $C_{S2} = 0.323$ pF, $L_{r1} = 4.37$ nH, $C_{r1} = 0.549$ pF, $L_{r2} = 5.73$ nH, $C_{r2} = 0.539$ pF, $L_{via} = 3.9$ nH, $L_N = 4.15$ nH, $C_N = 0.2$ pF.

with the maximum of -55 dB at 15.2 GHz. The overall stop-band attenuation is greater than 20 dB and is maintained up to 18.2 GHz. The horizontal slot improves the return loss characteristics. The designed filter exhibits a maximum insertion loss of 1.3 dB at 5.3 GHz and a minimum insertion loss of 0.6 dB at 3.5 GHz.

2.4. Equivalent Circuit Model

Figure 6 shows the equivalent circuit model that explains the transmission characteristics of the proposed UWB filter. The top and bottom metallic surfaces of SIW can be considered as a two-wire transmission line with an infinite number of short-circuited stubs called via walls. These vias are modelled as an inductor L_{via} . The CSRR is modelled as a parallel combination of capacitor C_r and inductor L_r . L_c and C_c indicate the inductive and capacitive coupling between the waveguide transmission line and CSRR, while L_s and C_s indicate the inductive and capacitive coupling between CSRRs. The circular CSRR in the ground is modelled as a series combination of inductor and capacitor, L_N and C_N respectively, which creates a notch band in the passband range. The coupling element values and via inductance are calculated using the following design equations (4), (5), and (6) then optimized by advanced design system (ADS).

$$L_C = \mu_0 \left(\frac{W_w}{2\pi} \right) \log \left[\csc \left(\frac{\pi L_M}{2W_w} \right) \right] \quad (4)$$

$$C_C = \varepsilon_0 \varepsilon_{eff} \left(\frac{2W_w}{\pi} \right) \log \left[\csc \left(\frac{\pi g}{2W_w} \right) \right] \quad (5)$$

$$L = 5.08h \left[\ln \left(\frac{4h}{d} \right) + 1 \right] \text{ nH} \quad (6)$$

where h indicates the height of the substrate, and d indicates the diameter of the vias. Figure 7 shows the comparison between EM and circuit simulations of the proposed SIW bandpass filter, which are carried out by CST and ADS software. The results

are in good agreement with the circuit simulation. The transmission zero at low frequencies is due to the external coupling between the SIW and resonators, and the coupling between the CSRRs results in transmission zero at high frequency.

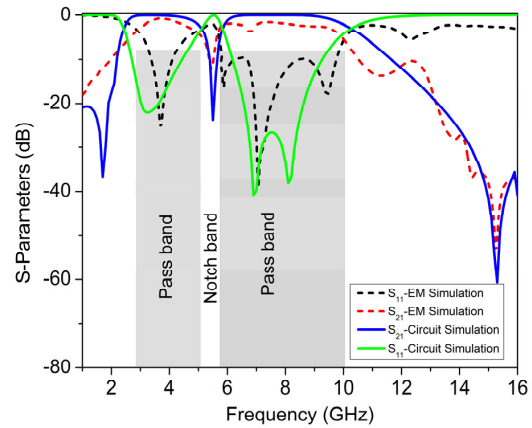


FIGURE 7. S parameter of circuit simulation and EM simulation.

2.5. Surface Current and Field Distribution

The surface current distribution at different frequencies is delineated in Figure 8. The current distribution at 1 GHz and 15 GHz indicates the stopband property of the bandpass filter as there is no current flow between port 1 to port 2 and vice versa. From this current distribution, a stopband at 1 GHz is created due to the evanescent mode characteristics of the filter, but at 15 GHz, attenuation is generated due to the triangular slot in the ground plane. The notch band creation from 5 GHz to 5.7 GHz due to the ground etched CSRR is depicted in Figure 8.

3. FABRICATION AND MEASUREMENT RESULTS

The fabricated prototype was measured using Anritsu-M2027C vector network analyzer. The measured results are in good agreement with the simulated ones (Figure 9), but the band-

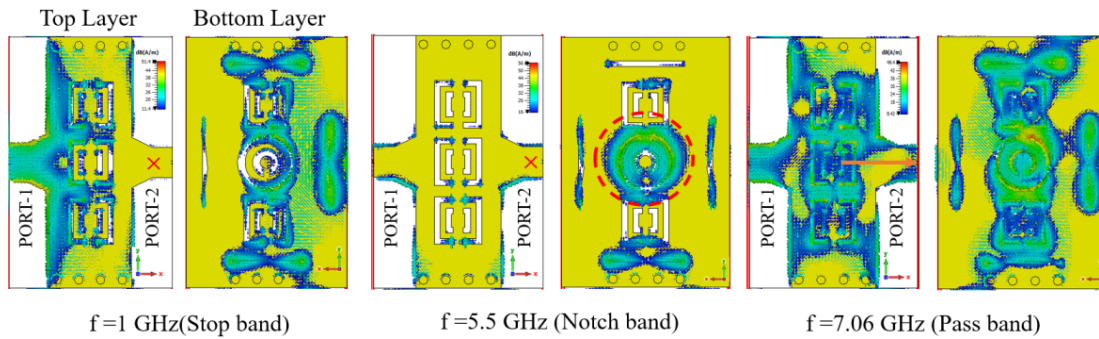


FIGURE 8. Surface current distribution for different frequencies.

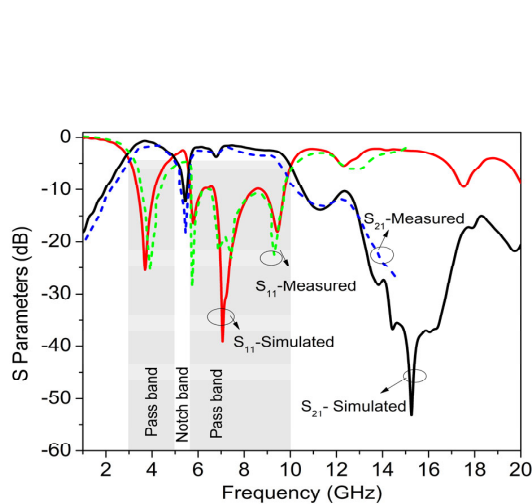


FIGURE 9. Simulated and measured S -parameter characteristics of proposed notch filter.

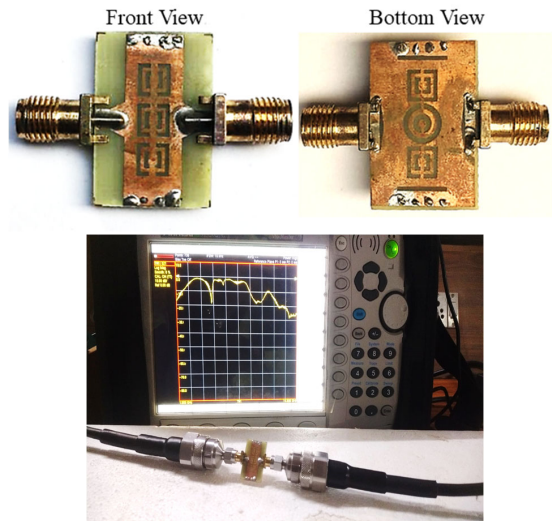


FIGURE 10. Fabricated prototype and measurement setup using Vector Network Analyzer (VNA).

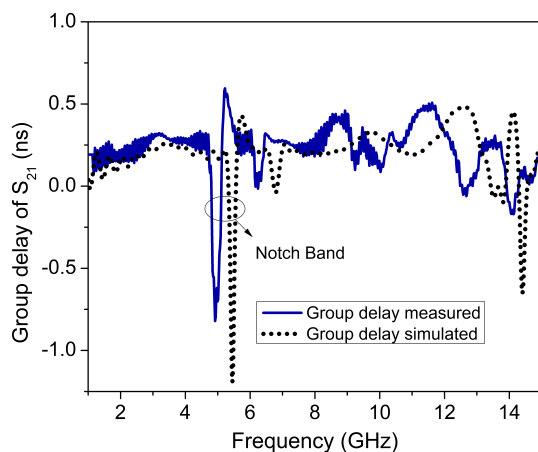


FIGURE 11. Simulated and measured group delay of proposed notch filter.

width varies due to the fabrication tolerance. The maximum return loss in the passband achieved is 30 dB. The proposed filter has a fractional bandwidth of 106% and notch bandwidth of 13% centered at 5.46 GHz with -18 dB insertion loss. Due to

the VNA frequency range limitations, measurements are performed up to 15 GHz. The small deviation in the measured results are due to the loss tangent of dielectric material and effect of SMA connector loss. The fabricated prototype and measurement setup are shown in Figure 10.

3.1. Group Delay

The group delay over the lower and upper passbands is almost constant. Figure 11 shows the simulated and measured group delays of a proposed filter. The measured maximum group delay in lower and upper passbands are 0.3 ns and 0.5 ns. Flat group delay is achieved over passband except the notch band, which indicates that the linearity between the input and output. The external quality factor can be calculated using Equation (7).

$$Q_e = \frac{\omega_0 \times \tau_{S_{11}}(\omega_0)}{4} \quad (7)$$

where $\tau_{S_{11}}(\omega_0)$ represents the group delay at passband mid-frequency (ω_0). The maximum variation in group delay is observed near the passband edges, which is caused by a sharp transition in the rejection level. The comparison of recently

TABLE 1. Comparison of UWB notch filter with previously reported literature.

Ref.	Passband (GHz) /Substrate	Size ($\lambda_{gL} * \lambda_{gW} = \lambda_g^2$) /Technique	No. of Notches	3 dB FBW NB (%)	Suppression Level	Stopband attenuation > 20 dB up to GHz
[2]	3.1–10.6/Taconic	0.514×0.31 /Microstrip	1	6.7	> 10	> 20 up to 25
[3]	3–10.75/Rogers TMM 10	0.45×0.79 /Microstrip	1	5.2	> 18	> 25 up to 15
[7]	3.1–10.6/Rogers5880	0.85×0.693 /Microstrip	1	5.7	> 20	> 10 up to 20
[8]	2.9–11.1/Rogers 5880	1.12×0.548 /Microstrip	1	9	> 10	> 15 up to 13
[9]	3.1–10.6/Taconic	2.03×0.53 /Microstrip	1	18	> 25	> 20 up to 12.5
[10]	3.1–10.6/Rogers 5880	1.275×0.56 /SIW	1	12	> 30	> 10 up to 14
This Work	2.9–10.3/FR-4	0.35×1.06 /SIW	1	12.9	> 14	> 25 up to 18

λ_g — guide wavelength at the center frequency of pass band. NB — Notch band.

published UWB bandpass filters (BPFs) with single notch band characteristics is given in Table 1. The proposed filter contributes high stopband characteristics with compact size.

4. CONCLUSION

A compact size ultra-wideband bandpass filter with notch-band characteristics is proposed and implemented. To obtain required ultra-wideband characteristics, a DSS-CSRR is employed on both top and bottom layers. Slots are etched in the ground layer to improve the performance characteristics of the filter by creating a transmission zero at the upper band edge. By etching a conventional CSRR on ground plane, a notch band ranging from 5 GHz to 5.7 GHz is obtained with insertion loss of 19 dB and fractional bandwidth of 12.9%. The measured results exhibit good passband characteristics with an insertion loss of less than 1.5 dB. Since the proposed filter contributes low insertion loss, it can be used for space applications.

REFERENCES

- [1] Bandyopadhyay, A., P. Sarkar, and R. Ghatak, "A bandwidth reconfigurable bandpass filter for ultra-wideband and wideband applications," *IEEE Transactions on Circuits and Systems II: Express Briefs*, Vol. 69, No. 6, 2747–2751, 2022.
- [2] Zhu, H. and Q.-X. Chu, "Ultra-wideband bandpass filter with a notch-band using stub-loaded ring resonator," *IEEE Microwave and Wireless Components Letters*, Vol. 23, No. 7, 341–343, 2013.
- [3] Yan, T., D. Lu, X.-H. Tang, and J. Xiang, "High-selectivity UWB bandpass filter with a notched band using stub-loaded multimode resonator," *AEU-International Journal of Electronics and Communications*, Vol. 70, No. 12, 1617–1621, 2016.
- [4] Xie, J., D. Tang, Y. Shu, and X. Luo, "Compact UWB BPF with broad stopband based on loaded-stub and C-shape SIDGS resonators," *IEEE Microwave and Wireless Components Letters*, Vol. 32, No. 5, 383–386, 2021.
- [5] Dong, Y. D., T. Yang, and T. Itoh, "Substrate integrated waveguide loaded by complementary split-ring resonators and its applications to miniaturized waveguide filters," *IEEE Transactions on Microwave Theory and Techniques*, Vol. 57, No. 9, 2211–2223, 2009.
- [6] Che, W., C. Li, K. Deng, and L. Yang, "A novel bandpass filter based on complementary split rings resonators and substrate integrated waveguide," *Microwave and Optical Technology Letters*, Vol. 50, No. 3, 699–701, 2008.
- [7] Ghatak, R., P. Sarkar, R. K. Mishra, and D. R. Poddar, "A compact UWB bandpass filter with embedded SIR as band notch structure," *IEEE Microwave and Wireless Components Letters*, Vol. 21, No. 5, 261–263, 2011.
- [8] Wei, F., L. Chen, X.-W. Shi, and C.-J. Gao, "UWB bandpass filter with one tunable notch-band based on DGS," *Journal of Electromagnetic Waves and Applications*, Vol. 26, 673–680, 2012.
- [9] Li, Q., Z.-J. Li, C.-H. Liang, and B. Wu, "UWB bandpass filter with notched band using DSRR," *Electronics Letters*, Vol. 46, No. 10, 692–693, 2010.
- [10] Li, Q. and T. Yang, "Compact UWB half-mode SIW bandpass filter with fully reconfigurable single and dual notched bands," *IEEE Transactions on Microwave Theory and Techniques*, Vol. 69, No. 1, 65–74, 2020.
- [11] Sarkar, D., T. Moyra, and L. Murmu, "An ultra-wideband (UWB) bandpass filter with complementary split ring resonator for coupling improvement," *AEU-International Journal of Electronics and Communications*, Vol. 71, 89–95, 2017.
- [12] Pendry, J. B., A. J. Holden, D. J. Robbins, and W. J. Stewart, "Magnetism from conductors and enhanced nonlinear phenomena," *IEEE Transactions on Microwave Theory and Techniques*, Vol. 47, No. 11, 2075–2084, 1999.
- [13] Falcone, F., T. Lopetegui, J. D. Baena, R. Marqués, F. Martín, and M. Sorolla, "Effective negative- ϵ stopband microstrip lines based on complementary split ring resonators," *IEEE Microwave and Wireless Components Letters*, Vol. 14, No. 6, 280–282, 2004.
- [14] Ali, A. and Z. Hu, "Metamaterial resonator based wave propagation notch for ultrawideband filter applications," *IEEE Antennas and Wireless Propagation Letters*, Vol. 7, 210–212, 2008.